# Development and investigation of novel nanoparticle embedded solutions with enhanced optical transparency

Rouholah Ashiri[a)]
*Department of Materials Science and Engineering, Dezful Branch, Islamic Azad University, P. O. Box 313, Dezful, Iran*

(Received 14 August 2014; accepted 21 October 2014)

The demands for highly transparent thin films for many integrated optical systems increase rapidly. The aim of the present work is to address these important needs. We show a novel approach for the nanocolloidal processing of barium titanate with enhanced optical transparency. The results showed that the stability of the prepared solution and optical transparency of the resulted thin film improved significantly. The study of the structure and properties of the prepared solutions indicated that the enhanced and homogenous transparency is due to the size-effect of the particles embedded in the solution, which are nanostructured. It seems to us that the proposed method has the capability of being a general strategy for obtaining highly transparent solutions and thin films. Moreover, the enhanced transparency of the prepared thin films can improve the energy efficiency of the solar power systems significantly.

## I. INTRODUCTION

Barium titanate is the most useful ferroelectric material.[1–9] Owing to their high refractive index, high transparency in the visible and near infrared wave length regions, wide band gap, and excellent chemical stability, barium titanate thin films can be used as anti-reflection coatings in solar cells, dielectric mirrors, and many other optical applications.[1,2] The use of alkoxides as precursors in the sol–gel process for the preparation of metal oxides powders and thin films has been explored with a view to nanostructuring.[1–7] However, the alkoxides, which are used in sol–gel preparation as precursors, are highly reactive compounds. Alkoxides tend to precipitate or age the sol.[7] This fact changes the nature of the sol, which in turn results in irreproducible optical properties of the resulted thin films.

Solar energy conversion is receiving increasing interest as a serious solution to energy production. A general trend in the optical and electro-optical devices is tendency toward miniaturization, which requires downsizing of raw materials.[3] The use of the nanosized starting materials for fabricating the multilayer integrated optical systems can reduce the device size.[4] Moreover, the preparation of the well-dispersed suspensions containing nanosized particles is a key knowledge for preparing the stabilized sol and is an emerging field in the recent researches.[10] Highly stable sol is the key requirement for preparing sol–gel thin films. Moreover, highly stable and well-dispersed solutions containing nanosized particles can exhibit unique optical transparency. In addition, downsizing the particles within the sol can result in downsizing the crystallite size of the resulted powders and thin films[11] and can improve the optical properties of the thin films. The physical properties of the sol–gel products are strongly influenced by the composition, method of preparation, and microstructural characteristics.[12,13] Moreover, understanding of the behavior of sols, especially the influence of chemistry, is a key factor for technical application in fabricating the thin films with reproducible and optimized properties. In a sol–gel dip-coating technique, the optical quality of the sol has a great effect on the optical properties of the prepared thin films. Since, the novel or modified methods of preparation can result in better optical response of the prepared thin films. Moreover, the problems from the hydrolysis and condensation of metal alkoxide reactants are usually encountered in the sol–gel processes.[14] In the course of investigating the means to alleviate these drawbacks, we have developed a novel sol–gel process to obtain $BaTiO_3$ precursor solutions and thin films with enhanced optical transparency. The enhanced transparency of the prepared thin films can significantly improve the energy efficiency of the solar power systems.

## II. EXPERIMENTAL PROCEDURE

A novel sol–gel derived $BaTiO_3$ solution with high stability was prepared by using glacial acetic acid (assay 100 pct; Merck, Whitehouse Station, NJ), barium acetate (assay > 99 pct; Merck), titanium tetra isopropyl alkoxide (TTIP) (assay > 98 pct; Merck), 2-propanol (assay > 99 pct; Merck), and deionized water as precursors. The optimal formulation of sol

[a)]Address all correspondence to this author.
e-mail: ro_ashiri@yahoo.com
DOI: 10.1557/jmr.2014.351

 © Materials Research Society 2014 

https://doi.org/10.1557/jmr.2014.351 Published online by Cambridge University Press

consists of acetic acid, barium acetate, TTIP, 2-propanol, and deionized water with 6:1:1:1:150 molar ratios, respectively. The preparation method will be discussed in detail later. Ultrathin amorphous films were obtained using a sol–gel dip-coating technique under particular experimental conditions: the speed of drawing out from the solution was 1 cm/min, the calcination temperature was 773 K (500 °C) for 1 h, and the used substrate was a soda lime glass. The fired film thickness was 30 nm. Topography and root mean square (RMS) roughness of the prepared thin film were determined by an atomic force microscopy (AFM) (Thermo Microscopes; Auto probe CP Research) technique. In this evaluation, the studied surface was equal to 1 μm × 1 μm in area. The AFM results showed that the RMS roughness of the prepared thin film was quite small and equal to 0.743 nm.

Optical spectroscopy of barium titanate sols and thin films and Fourier transform infrared (FTIR) spectroscopy analysis of sols were performed using UV–visible spectrophotometer Hitachi 3410 and Bruker (Vector 33) instruments, respectively. The film thickness was measured by using Veeco Dektak 150 Profilometer (Oyster Bay, NY). The Dektak 150 is a surface profilometer used for surface measurements using contact profilometry techniques and can provide down to a step height measurement of 2 angstroms. The microstructure of the particles embedded in the sol and thin films was characterized by using transmission electron microscopy (TEM, Philips CM200, Almelo, Netherlands, operated at 100 kV) and scanning electron microscopy (SEM, Philips XL31) techniques.

## III. RESULTS AND DISCUSSIONS

In the sol–gel method, the cost of used materials and processing time are the key parameters that we tried to optimize. The great sensitivity of titanium alkoxides to hydrolysis makes their sol–gel transformation very fast and thus difficult to control. A two-step and discontinuous hydrolysis process was developed using alcohol and water aided by low-temperature processing to control the rate of a hydrolysis process. It was found that the dilution of titanium alkoxide with a solvent such as a suitable alcohol could decrease its reactivity. In the first step, introducing the alcohol (2-propanol) to the mixture reduced the rate of the hydrolysis. This fact is due to the presence of ligands surrounding the alkoxide and controls its reactivity. Considering the above facts, a new method of preparation was introduced in the present work. The flowchart of the method is shown in Fig. 1. In this flowchart, the black-colored boxes indicate the used precursors and related ratios. The violet and green-colored boxes are processing steps, aiming to homogenize the mixture and to control the size of the formed species.

There are several differences between our method and other established methods.[15–21] In the proposed method, to control the hydrolysis process and sol–gel transformation, more attention was focused on the hydrolysis process and a two-step hydrolysis process was used. The preparation costs significantly decreased because a much lower amount of 2-propanol and acetic acid was used, and no modifier such as acetyl acetone was used.[21] In contrast to other reported methods,[15,16] quick preparation is other advantage of the method of preparation because the sol is prepared only in 90 min, and the time required for xerogel calcination is only 1 h, which is more desirable from an economical point of view. One of the main differences between the present method and other established methods[19,20] is use of nanoscaled building blocks for the preparation of the final products. To reach this, a low-temperature hydrolysis process (the orange-colored box in Fig. 1) was designed to modify the preparation method for the first time. The mentioned hydrolysis process, which results in the production of nanoscale chemical species within the sol, can control the rate of the sol–gel reactions. The size-effect resulted from modification of the preparation process is the reason behind the homogenous and enhanced optical response of the products. At lower temperature, the reaction rate decreases. As another controlling parameter, the reduction of temperature in the initial stage of mixing of precursors (see the violet-colored boxes in Fig. 1) can control the size of the forming species and accordingly, it can improve the stability and optical transparency of the obtained sol. Moreover, the visual inspection of the sol prepared through our proposed method indicated that the stability of the sol increased twice with a decrease in the temperature. The FTIR spectrum of the solution prepared through our proposed method was compared with that of the solution prepared at room temperature as shown in Fig. 2. By using this figure, the reaction mechanisms in the sol–gel process can be detected. Chemical bonds vary widely in their sensitivity to probing by infrared techniques. The fundamental theory of infrared spectroscopy delineates a band shape analysis. Three characteristics are commonly examined: peak position, integrated peak intensity, and peak width. The peak position is most commonly exploited for qualitative identification because each chemical functional group displays peaks at a unique set of characteristic frequencies. This provides a fingerprint that can be used to identify chemical groups. Moreover, the integrated intensity is proportional to the concentration of absorbing bonds.[16] Figure 2 indicates that the intensity of peaks in the spectrum of the solution prepared through our proposed procedure is rather low compared with the spectrum of the solution prepared at higher (room) temperature. This fact indicates that the concentration of the corresponding bonds is higher in

https://doi.org/10.1557/jmr.2014.351 Published online by Cambridge University Press

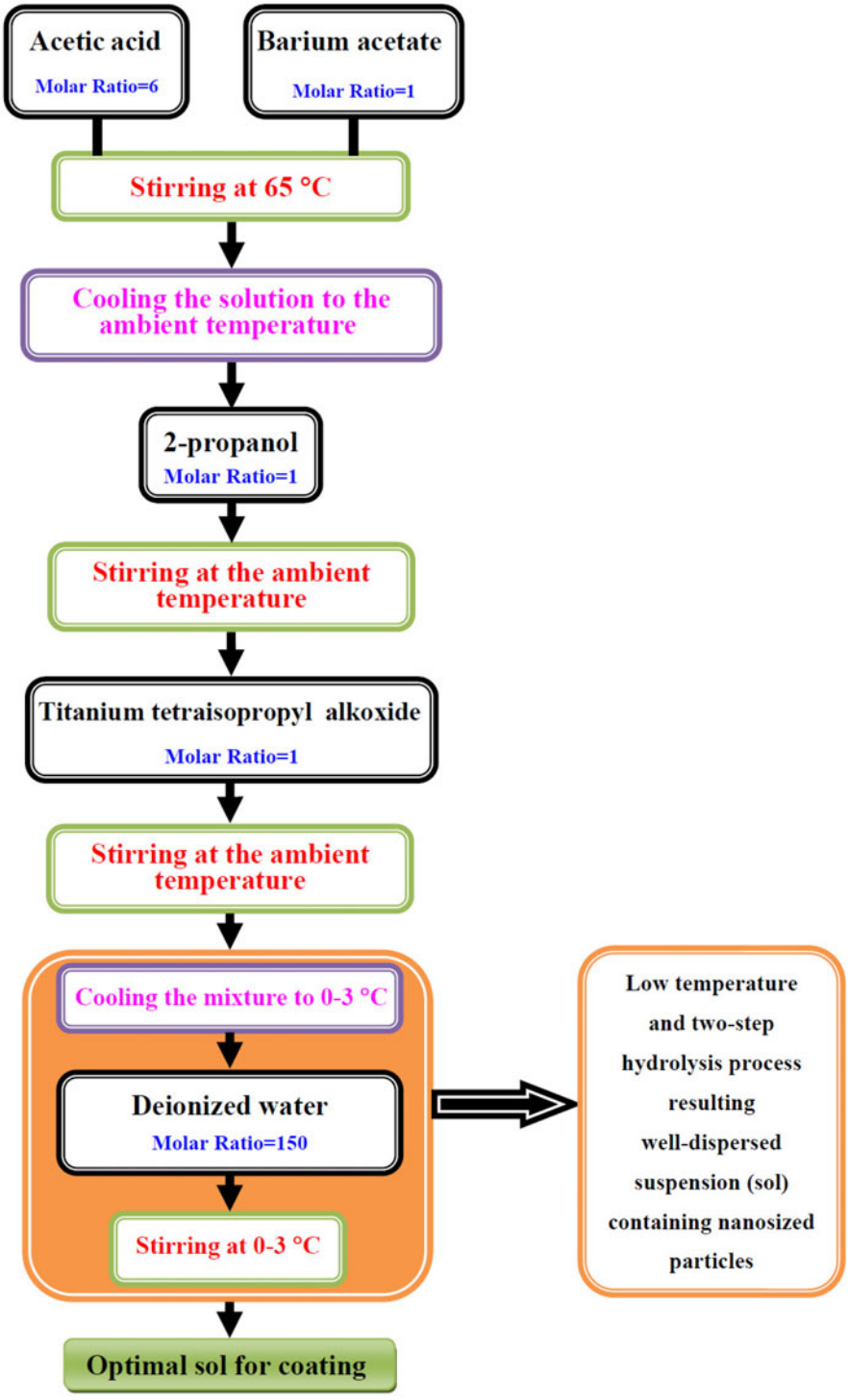



FIG. 1. Flowchart showing the method of preparation of the solutions.

the solution prepared at room temperature. In other words, the rate of sol–gel reactions is more rapid at higher temperature. However, at higher temperatures there are more colliding species, which have the necessary activation energy resulting in more successful collisions and an increased reaction rate. This fact accelerates the rate of the sol to gel evolution and therefore reduces the stability of the sol. Highly stable sol is the key requirement for the preparation of the sol–gel thin films. The characteristic absorption band of the used alkoxide appears at 1000 $cm^{-1}$. This absorption band does not appear in the spectra of Fig. 2, indicating the initiation of the hydrolysis process. However, the rate of hydrolysis reactions is higher in the sample prepared at higher temperature. The analysis

https://doi.org/10.1557/jmr.2014.351 Published online by Cambridge University Press

and assignment of the absorption bands present in Fig. 2 are described in Table I. In contrast to the spectrum of the solution prepared through our method [Fig. 2(a)], two events occurred in the spectrum of the solution prepared at ambient temperature [Fig. 2(b)]:

(i) Increase in the absorption band intensity and decrease in their width: If no bonds are created or destroyed, the absorption band intensity is proportional to the concentration of absorbing bonds.

(ii) Appearance of some new absorption bands (including bands, which appear at 618, 1138, and 1733 $cm^{-1}$). This event that was seen at higher temperatures is due to new functional groups. This fact also indicates the progress of the sol–gel reactions.

According to the mass effect law, the rate of a reaction can be affected by the concentration of reactant species and kinetic constant of the reaction. The higher reaction temperature increases the concentration of the reactant species. Moreover, the kinetic constant of reaction increases exponentially with the temperature according to the following equation:[22]

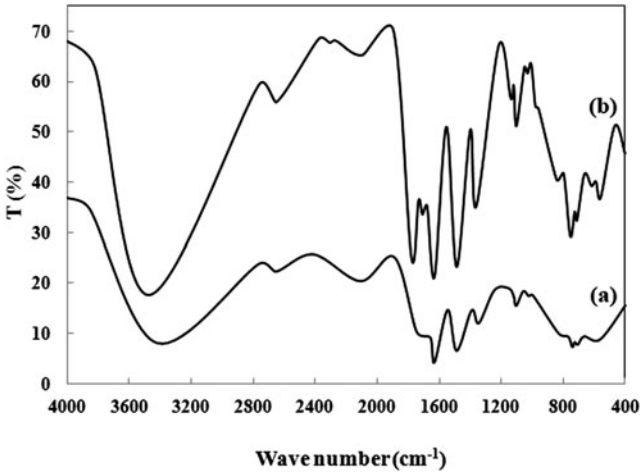



FIG. 2. FTIR spectra of sol–gel solutions prepared (a) through our method and (b) at room temperature.

$$k = A \exp\left(-\frac{Q}{RT}\right) \quad , \tag{1}$$

where $k$ is the kinetic constant, $Q$ is the activation energy, and $A$ and $R$ are constants. In other words, the higher reaction temperature increases the number and size of the particles embedded in the solution. An increase in the size of the particles is also accompanied by a decrease in the optical transparency of the prepared sol and thin films. The fact is the reason behind utilizing the lower temperature in our proposed method. The absorption spectrum of the solution prepared through our proposed method was compared with that of the solution prepared at room temperature as shown in Fig. 3. This figure clearly confirms the above discussion indicating the growth of the particles embedded in the sol with an increase in processing temperature. According to the Beer–Lambert law, the absorbance is proportional to the concentration and size of the absorbing particles within the sol. Particle size has opposing impacts on the transmittance; a larger particle increases forward scattering but also absorbs more.[23] The great difference between two absorption spectra presented in Fig. 3 clearly indicates that the improvement made by our method is significant. As the most important characteristic of our method, downsizing of the particles embedded in the sol to the nanometric scale significantly improved the optical transparency of the sol and thin film. This fact makes our preparation method attractive and potentially very useful for many optical applications such as solar power systems, UV shielding equipments, antireflective coatings, optical lenses, and dielectric mirrors.

It has been mentioned that stable solutions are required to be used in industrial coating technology.[23] The nature of unstable sol–gel solutions changes with time and therefore, their products do not exhibit similar properties. This fact is due to the progress in the sol–gel reactions. Structure and shape of the particles embedded in the sol depend strongly on the kind and ratio of the precursors

TABLE I. Origin of relevant infrared absorption frequencies (which have appeared in the spectra of Fig. 2) of the sol–gel derived solutions.

| Sample description | Peak position ($cm^{-1}$) | Mode of vibration | Originated from | Ref. |
|---|---|---|---|---|
| Sol–gel derived solutions | 3479 and 3421 | O–H stretching vibration in water | Presence of water in the xerogel | 1–4 |
| | 2650 | C–H stretching vibration mode | Presence of $–CH_2$ and $–CH_3$ functional groups that are due to the alkoxide | 1–4 |
| | 1780 | Asymmetric [$\nu_{as}$(COO−)] stretching vibrations of carboxylate groups | Presence of acetate groups bonded to barium atoms | 1–4 |
| | 1678 | O–H stretching vibration in alcohol | Presence of alcohol (2-propanol) in the xerogel | 1–4 |
| | 1487 | Symmetric [$\nu_s$(COO−)] stretching vibrations of carboxylate groups | Presence of acetate groups bonded to barium atoms | 1–4 |
| | 1361, 1138, 1102, 1050, and 842 | C–H bending vibration mode | Presence of alcohol (2-propanol) in the xerogel | 1–4 |
| | Wave numbers smaller than 800 | Ti–O vibration modes | Ti–O and Ti–O–Ti vibrations | 1–4 |

https://doi.org/10.1557/jmr.2014.351 Published online by Cambridge University Press

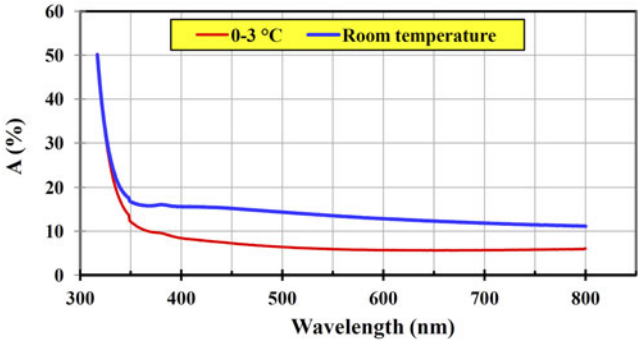



FIG. 3. Effect of the processing temperature on the UV–Vis–NIR absorption spectra of the sol–gel derived solutions.

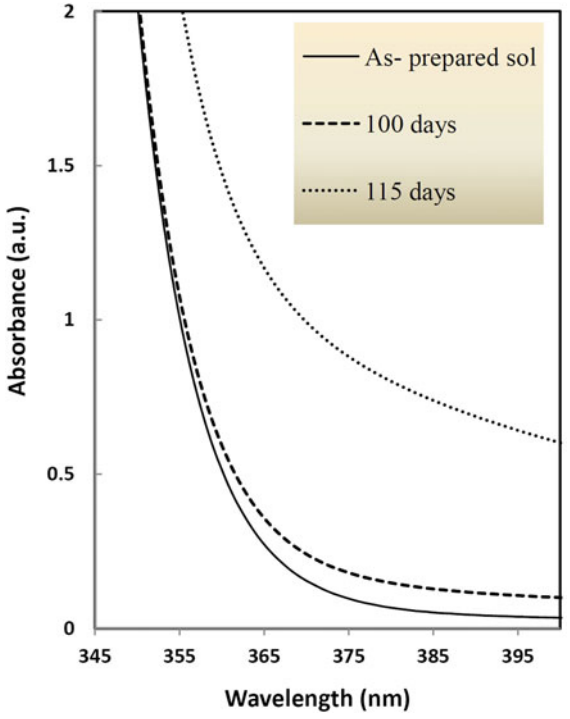



FIG. 4. The change in the absorption spectrum of the as-prepared sol with time.

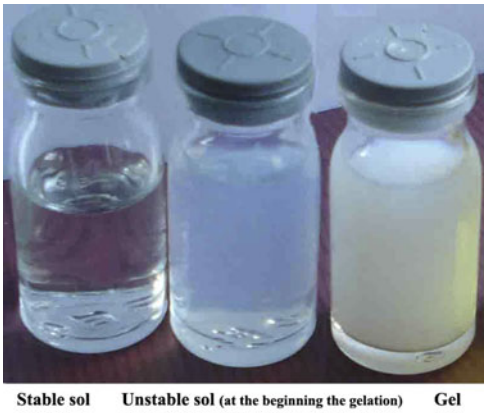



FIG. 5. The images of sol to gel evolution (sol aging) showing stable sol, which is colorless, unstable sol, and gel.

and processing conditions. In addition, the reaction conditions determine the size of the sol particles as well as their structure. Moreover, the change in the nature of the prepared sol changes the quality and structure of the prepared thin films. This fact will result in an irreproducible optical response of the prepared thin films. Our proposed method can control the rate of the sol–gel reactions and can be used to prepare highly stable sol for coating application. Monitoring of the absorption spectra of the prepared solution indicates that the prepared sol was stable for more than 100 days. Figure 4 shows the absorption spectrum of the as-prepared sol and absorption spectra of the same sol after 100 and 115 days. This figure indicates that the change in the absorption spectrum of the as-prepared sol in 100 days is negligible but a significant change occurs in 115 days. This fact indicates that the particles imbedded in the sol tend to grow very fast after 100 days. The tendency of the growing particles to absorb the emitted light is more than small particles. This fact is the reason behind the great difference between absorption spectra after 100 and 115 days. The visual inspection indicated that the as-prepared sol is colorless and remains colorless for 100 days. After 100 days, the sol slowly changes its color to bluish and its viscosity increases as well. This fact is due to the fast progress of the polycondensation reactions. After 115 days, the sol to gel transformation occurs for 4 days (see Fig. 5). These facts confirm the results presented in Fig. 4. The as-prepared sol, which is shown in Fig. 5, was colorless due to the presence of ultrafine nanoparticles in the sol, which have a lower tendency to absorb the incurred light. The unstable or overaged sol contains the larger particles. The growth of the particles embedded in the sol is due to the progress of the sol–gel reactions. Particle size has opposing impacts on the transmittance; a larger particle increases forward scattering but also absorbs more. This fact changes its color to bluish (see Fig. 5). After this stage, the growing particles or condensed species link together to become a 3-D network. In other words, as condensation reactions progress, the sol will set into a rigid gel.

The main application of the proposed method of preparation is for applications needing high transparency in the visible range. The enhanced transparency of the prepared thin films can significantly improve the energy efficiency of the solar power systems. Especially in solar cells (see the schematic of Fig. 6), there are permanent demands for highly transparent and antireflective layers. Moreover, ferroelectric materials exhibit photovoltaic effects under near-ultraviolet illumination. The most outstanding advantage of the photovoltaic effect of a

https://doi.org/10.1557/jmr.2014.351 Published online by Cambridge University Press

ferroelectric material is its high output voltage over 1 kV.[24] In Fig. 7, the transmission spectrum of the nanothin film prepared through the present method has been shown. This figure indicates that the optical propagation losses of $BaTiO_3$ thin films are much lower than the optical propagation losses of the similar works.[18,19,25] This figure also shows the enhanced optical transparency of the prepared thin film compared with other works and indicates the importance and significant improvement made by our method. Moreover, the homogeneity of the optical quality is evident from the spectrum of the thin film prepared with our approach. The transmission spectrum of the prepared thin films does not exhibit successive maxima and minima, which have appeared in the spectra of the thin films prepared by Dube et al.[18] and Pencheva et al.[25] The homogenous and high-level of transparency of the thin film prepared through the method developed in this work can be used for several applications. In the next paragraph, the better optical transparency of the prepared sol will be discussed.

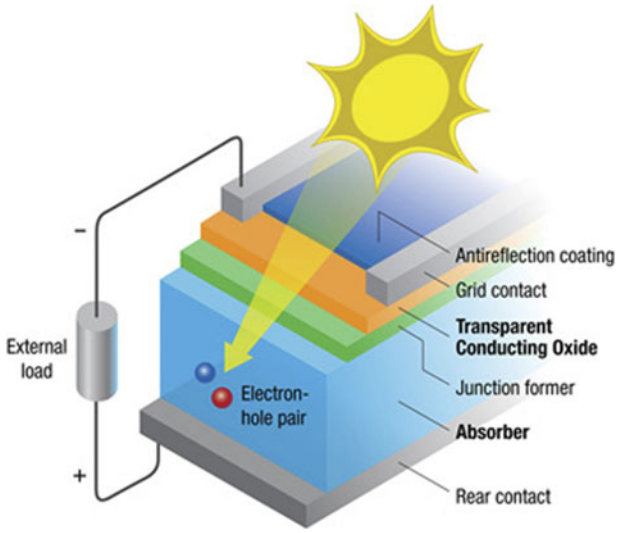



FIG. 6. Schematic diagram of a solar cell integrated system.

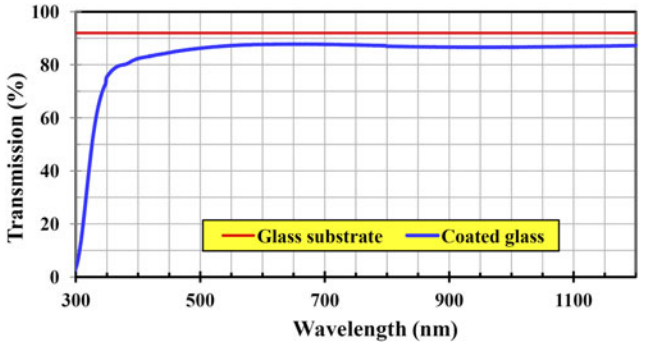



FIG. 7. UV–Vis–NIR transmission spectrum of the prepared nanothin film.

New strategies for materials' fabrication are of fundamental importance in the advancement of science and technology.[1–4,26–33] Microstructures are the strategic links between materials' processing and materials' behaviors. Therefore, microstructures are at the center of materials science and engineering and consequently, microstructure control is essential for any processing activity. It seems to us that the enhanced optical transparency of the prepared sol and thin film is due to the size-effect of the particles imbedded in the sol. Figure 8 shows the TEM micrograph of a particle imbedded in the sol, which was prepared through our established method. This figure also shows that the prepared sol consists of regularly shaped near spherical particles. According to Fig. 7, it can be seen that the deposited thin film is highly transparent in the wave length range from 400 to 1200 nm with an average transmission of 87%, which is higher than the previous reported value in similar researches; in those, the average value in the range of 70–75% was reported.[17,18,34] As we know, the energy of incident light on a transparent material is divided into two sections. The first fraction transmits through the material and the other is the losses that are incurred by absorption and reflection.[1] Beer–Lambert law states that there is a logarithmic dependence between the transmission of light through a substance, $T$, and its absorption coefficient, $\alpha$.[1] An increase in the size of absorbing species results in increment of the absorption losses. Therefore, downsizing the particles embedded in the sol to the nanometric scale can significantly improve the optical properties of the thin films and can lead to a significant decrease in the fraction of the absorbed light. This fact is the reason behind the high transparency quality of the sol–gel derived solutions and thin films.

The above-discussed thin films were amorphous. A significant decrease in the transparency of the thin films is seen when the amorphous thin films crystallize. Figures 9 and 10 show the transmission spectra, microstructure, and topography of the nanostructured barium

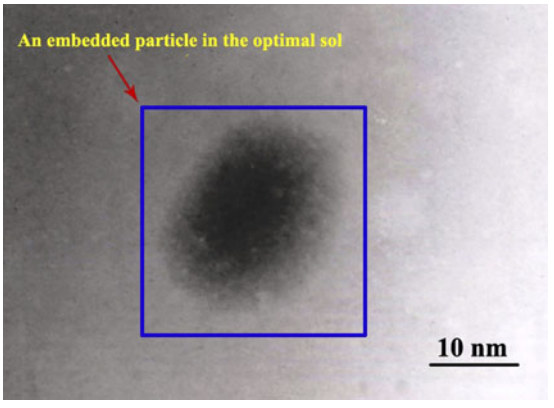



FIG. 8. TEM micrograph of one of the formed species (a sol particle) in the optimal sol.

https://doi.org/10.1557/jmr.2014.351 Published online by Cambridge University Press

titanate thin films deposited on fused silica substrates at different calcination temperatures. Figure 9 indicates that the transmittance decreases with an increase in the calcination temperature. During the calcination process, the volatile materials in the gel film gradually evaporate. This fact increases the density of the annealed thin films in contrast to the as-coated films, which is accompanied by the reduction in the intensity of the transmitted light. This fact is the reason behind the reduction of the transmittance with an increase in the calcination temperature. Moreover, Fig. 10 indicates that the obtained thin films are nanocrystalline. Another fact reducing the transmittance is the progress of the nanothin films in the direction of crystallization with the increase of the calcination temperature.

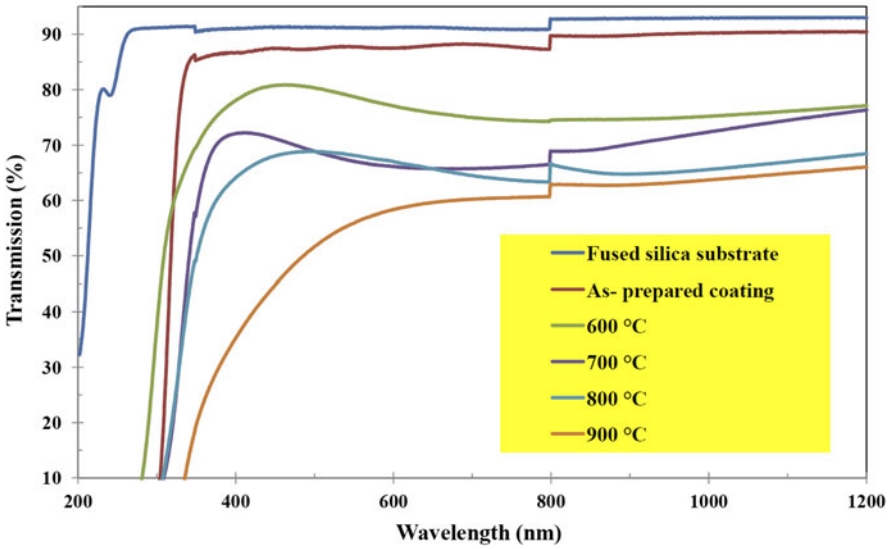



FIG. 9. UV–Vis–NIR transmission spectra of the nanostructured barium titanate thin films deposited on fused silica substrates at different calcination temperatures.

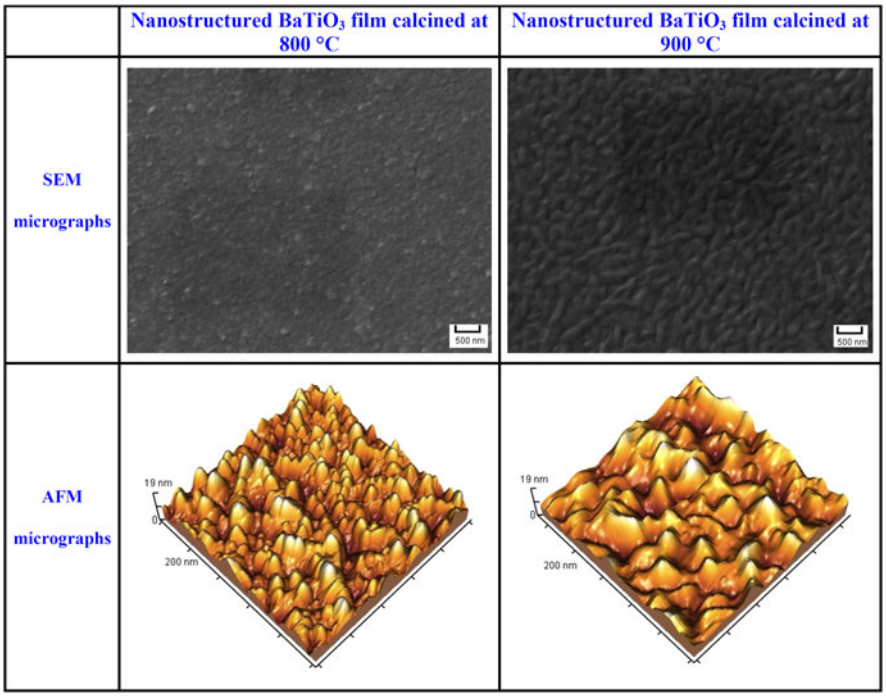



FIG. 10. SEM and 3D AFM micrographs of the nanostructured barium titanate thin films deposited on fused silica substrates at different calcination temperatures.



https://doi.org/10.1557/jmr.2014.351 Published online by Cambridge University Press

## IV. CONCLUSIONS

We show a novel approach for colloidal processing of barium titanate with enhanced optical transparency. The results showed that the stability of the prepared solution and optical transparency of the resulted thin film significantly improved. The study of the structure and properties of the prepared solutions indicated that the enhanced and homogenous transparency is due to the size-effect of the particles embedded in the solution. Compared to other approaches, the overall procedure used in this work was very simple, cost-effective, and environmentally friendly.

## REFERENCES


1. R. Ashiri, A. Nemati, M. Sasani Ghamsari, and H. Adelkhani: Characterization of optical properties of amorphous $BaTiO_3$ nanothin films. *J. Non-Cryst. Solids* **355**, 2480 (2009).
2. R. Ashiri, A. Nemati, M. Sasani Ghamsari, S. Sanjabi, and M. Aalipour: A modified method for barium titanate nanoparticles synthesis. *Mater. Res. Bull.* **46**, 2291 (2011).
3. R. Ashiri: Analysis and characterization of phase evolution of nano-sized $BaTiO_3$ powder synthesized through a chemically modified sol–gel process. *Metall. Mater. Trans. A* **43**, 4414 (2012).
4. R. Ashiri: Detailed FTIR spectroscopy characterization and thermal analysis of synthesis of barium titanate nanoscale particles through a newly developed process. *Vib. Spectrosc.* **66**, 24 (2013).
5. Y.F. Joya and Z. Liu: Formation of ultraviolet laser-annealed mesoporous anatase films by a sol–gel process. *Scr. Mater.* **60**, 467 (2009).
6. N. Lecerf, S. Mathur, H. Shen, M. Veith, and S. Hüfner: Chemical vapour and sol–gel syntheses of nano-composites and -ceramics using metal-organic precursors. *Scr. Mater.* **44**, 2157 (2001).
7. D. Sporn: *Chemical Physics of Thin Film Deposition for Micro- and Nano-Technologies* (Springer, Netherlands, 2002).
8. J. Zhao, X. Wang, R. Che, and L. Li: Dispersion of barium titanate in aqueous media. *Ceram. Int.* **33**, 207 (2007).
9. P. Yu, X. Wang, and B. Cui: Preparation and characterization of $BaTiO_3$ powders and ceramics by the sol–gel process using organic monoacid as surfactant. *Scr. Mater.* **57**, 623 (2007).
10. G.H. Hsiue, L.W. Chu, and I.N. Lin: Optimized phosphate ester structure for the dispersion of nano-sized barium titanate in proper non-aqueous media. *Colloids Surf., A* **294**, 212 (2007).
11. W. Chen, J. Zhang, Q. Fang, S. Li, J. Wu, F. Li, and K. Jiang: Sol–gel preparation of thick titania coatings aided by organic binder materials. *Sens. Actuators, B* **100**, 195 (2004).
12. R. Gupta, S. Mozumdar, and N.K. Chaudhury: Effect of ethanol variation on the internal environment of sol–gel bulk and thin films with aging. *Biosens. Bioelectron.* **21**, 549 (2005).
13. S. Tangwiwat and S.J. Milne: Barium titanate sols prepared by a diol-based sol–gel route. *J. Non-Cryst. Solids* **351**, 976 (2005).
14. W.K. Kuo, B. Lo, and Y.C. Ling: Steric stabilization of sol–gel prepared $BaTiO_3$ precursors with nonylphenoxypolyethoxyethanol. *Mater. Chem. Phys.* **60**, 132 (1999).
15. X. Xing, J. Deng, J. Chen, and G. Liu: Phase evolution of barium titanate from alkoxide gel-derived precursor. *J. Alloys Compd.* **384**, 312 (2004).
16. B. Lee and J. Zhang: Preparation, structure evolution and dielectric properties of $BaTiO_3$ thin films and powders by an aqueous sol–gel process. *Thin Solid Films* **388**, 107 (2001).
17. M. Burgos and M. Langlet: The sol–gel transformation of TIPT coatings: A FTIR study. *Thin Solid Films* **349**, 19 (1999).
18. R. Thomas, D.C. Dube, M.N. Kamalasanan, and S. Chandra: Optical and electrical properties of $BaTiO_3$ thin films prepared by chemical solution deposition. *Thin Solid Films* **346**, 212 (1999).
19. O. Harizanov and A. Harizanova: Formation and characterization of sol–gel barium titanate. *Mater. Sci. Eng., B* **106**, 191 (2004).
20. M. Nenkov and T. Pencheva: Investigation of inhomogeneity of $BaTiO_3$ thin films using transmittance spectra measurements. *Thin Solid Films* **324**, 305 (1998).
21. O.A. Harizanov: Sol–gel $BaTiO_3$ from a peptized solution. *Mater. Lett.* **34**, 232–236 (1998).
22. SKh. Sadrnejad: *Kinetic Process in Materials Engineering and Metallurgy* (Amirkabir Publishing Crop, Tehran, 2004).
23. O. Harizanov and A. Harizanov: Development and investigation of sol–gel solutions for the formation of $TiO_2$ coatings. *Sol. Energy Mater. Sol. Cells* **63**, 185 (2000).
24. W. Cai, Ch. Fu, J. Gao, Q. Guo, X. Deng, and Ch. Zhang: Preparation and optical properties of barium titanate thin films. *Phys. B* **406**, 3583 (2011).
25. T. Pencheva and M. Nenkov: Optical inhomogeneity of $BaTiO_3$ thin films and its correlation with some deposition conditions. *Vacuum* **58**, 374 (2000).
26. R. Ashiri, A. Nemati, and M. Sasani Ghamsari: Crack-free nanostructured $BaTiO_3$ thin films prepared by sol–gel dip-coating technique. *Ceram. Int.* **40**, 8613 (2014).
27. R. Ashiri: Analysis and characterization of relationships between the processing and optical responses of amorphous $BaTiO_3$ nanothin films obtained by an improved wet chemical process. *Metall. Mater. Trans. B* **45**, 1472 (2014).
28. R. Ashiri: A mechanistic study of nanoscale structure development, phase transition, morphology evolution, and growth of ultrathin barium titanate nanostructured films. *Metall. Mater. Trans. A* **45**, 4138 (2014).
29. R. Ashiri, A. Moghtada, A. Shahrouzianfar, and R. Ajami: Low temperature synthesis of carbonate-free barium titanate nanoscale crystals: Toward a generalized strategy of titanate-based perovskite nanocrystals synthesis. *J. Am. Ceram. Soc.* **97**, 2027 (2014).
30. F. Davar, M.R. Loghman-Estarki, and R. Ashiri: From inorganic/organic nanocomposite based on chemically hybridized CdS–TGA to pure CdS nanoparticles. *J. Ind. Eng. Chem.* **21**, 965 (2015).
31. F. Davar, M.R. Loghman-Estarki, M. Salavati-Niasari, and R. Ashiri: Synthesis of volcano-like CdS/organic nanocomposite. *Int. J. Appl. Ceram. Technol.* **11**, 637 (2014).
32. R. Ashiri, A. Moghtada, and R. Ajami: Sonochemical synthesis of $SrTiO_3$ nanocrystals at low temperature. *Int. J. Appl. Ceram. Technol.* DOI:10.1111/ijac.12315, in press.
33. R. Ashiri and A. Moghtada: Carbonate-free strontium titanium oxide nanosized crystals with tailored morphology: Facile synthesis, characterization and formation mechanism. *Metall. Mater. Trans. B* **45**, 1979 (2014).
34. H.X. Zhang: Optical and electrical properties of sol–gel derived $BaTiO_3$ films on ITO coated glass. *Mater. Chem. Phys.* **63**, 174 (2000).


https://doi.org/10.1557/jmr.2014.351 Published online by Cambridge University Press